Time-Resolved Diffuse Optical Spectroscopy up to 1700 nm by Means of a Time-Gated InGaAs/InP Single-Photon Avalanche Diode

Ilaria Bargigia,[a,*] Alberto Tosi,[b] Andrea Bahgat Shehata,[b] Adriano Della Frera,[b] Andrea Farina,[c] Andrea Bassi,[a] Paola Taroni,[a,c] Alberto Dalla Mora,[a] Franco Zappa,[b] Rinaldo Cubeddu,[a,c] Antonio Pifferi[a,c]

[a] *Politecnico di Milano, Dipartimento di Fisica, Piazza Leonardo da Vinci 32, 20133 Milano, Italy*
[b] *Politecnico di Milano, Dipartimento di Elettronica e Informazione, Piazza Leonardo da Vinci 32, 20133 Milano, Italy*
[c] *Consiglio Nazionale delle Ricerche, Istituto di Fotonica e Nanotecnologie, Piazza Leonardo da Vinci 32, 20133 Milano, Italy*

We present a new compact system for time-domain diffuse optical spectroscopy of highly scattering media operating in the wavelength range from 1100 nm to 1700 nm. So far, this technique has been exploited mostly up to 1100 nm: we extended the spectral range by means of a pulsed supercontinuum light source at a high repetition rate, a prism to spectrally disperse the radiation, and a time-gated InGaAs/InP single-photon avalanche diode working up to 1700 nm. A time-correlated single-photon counting board was used as processing electronics. The system is characterized by linear behavior up to absorption values of about 3.4 cm^{-1} where the relative error is 17%. A first measurement performed on lipids is presented: the absorption spectrum shows three major peaks at 1200 nm, 1400 nm, and 1700 nm.

Index Headings: **Time-resolved spectroscopy; Turbid media; Photon migration; Supercontinuum; Single-photon avalanche diode; SPAD; InGaAs/InP.**

INTRODUCTION

Optical spectroscopy of turbid media is exerting a growing appeal in medicine, biology, and in the fields of quality assessment of food and pharmaceutical products, thanks to its capability of noninvasively characterizing a variety of highly diffusive materials.

Even though in the spectral region beyond 1100 nm strong differences are expected to occur among different tissues and structures, in this range there is still little data available for the absorption and scattering properties of turbid media in the field of diffused optics and in particular for what concerns time-resolved measurements. Moreover, important constituents both of biomedical interest and attractive for non-biomedical applications may show a more marked relevance above 1100 nm rather than below this limit. Examples of important materials could be collagen, glucose, and hydroxyapatite for the biomedical field and starch, lignin, and cellulose for other applications. Covering the range between 600 nm and 1100 nm, few broadband spectroscopy systems have been developed based on multidistance continuous wave (CW) illumination,[1,2] on a combination of frequency domain measurements operated at a few discrete wavelengths and a spectral CW acquisition,[3,4] or on time-domain techniques.[5] Only recently, a system based on multidistance CW illumination able to perform measurements up to 1600 nm has been implemented and the absorption coefficients of lipids have been recovered.[6] Another group performed measurements on a human forearm in the region 1150–1520 nm using diffuse reflectance measurements in CW.[7]

Time-domain approaches are particularly appealing because of the possibility of effectively uncoupling absorption and scattering effects.[8] In fact, absorption and scattering affect differently the temporal distribution of re-emitted photons related to the multiple random paths experienced by photons in the medium. Furthermore, they permit the extraction of few signal photons out of a huge background, if uncorrelated. The problem of performing broadband time-resolved spectroscopy measurements is not trifling: first a pulsed laser source tunable over a broad spectral range is needed, then a wide dynamic range and the ability to control light power at individual wavelengths are required to account for the large changes in the optical signal experienced in a broad spectral range. In addition, exploring the spectral region beyond 1100 nm is particularly challenging: in most conditions of practical interest the optical signal is strongly attenuated due to the high absorption of water, the pulse temporal broadening is severely contracted, and a general decrease in sensitivity is observed. To overcome these problems, systems with sensitivity down to the single-photon level and a good temporal resolution are essential. These difficulties are probably the reason time-resolved diffuse optical spectroscopy has been performed mostly in the 600 to 1000 nm range, with a few pilot works up to 1100 nm and no broadband in vivo studies beyond this wavelength. A first example of time-domain spectral measurement was implemented using a supercontinuum source generated by a high peak power (in the Terawatt range) laser focused into a nonlinear medium and a streak camera as detection system;[9] other solutions were based either on tunable mode-locked lasers with time-correlated single-photon counting (TCSPC) electronics[10] or on the generation of supercontinuum radiation by means of a high repetition rate laser focused into a photonic crystal fiber, combined either with a streak camera[11] or with a TCSPC system.[12] A system performing measurements up to 1300 nm, even though with much lower temporal resolution, was demonstrated and applied to wood samples;[13] only quite recently, a first tunable time-resolved device working up to 1400 nm has been developed:[14,15] it is based on a supercontinuum laser source and a cooled micro-channel plate (MCP) photomultiplier tube.

Detectors with high efficiency, low dark count rate, low time

Received 30 August 2011; accepted 8 May 2012.
* Author to whom correspondence should be sent. Author E-mail: ilaria.bargigia@mail.polimi.it.
DOI: 10.1366/11-06461

0003-7028/12/6608-0944$2.00/0

jitter, and the possibility of fast time-gating (to further limit noise by keeping the detector OFF before and after the arrival time of photons to be detected) are required to perform effective measurements.[16] However, this is not easily achieved at long wavelengths. Micro-channel plate PMTs (MCP-PMTs)[17] for the near-infrared wavelength range (up to 1700 nm) display a low detector time jitter (less than 100 ps at full width at half-maximum (FWHM))[18] and wide active areas with diameters of about 2 mm; conversely their detection efficiency is low (less than 1%). Streak cameras[19] have very good timing resolution, with a jitter of a few picoseconds (ps), but have low sensitivity and small dynamic range and are very expensive. When operated at cryogenic temperatures (2.4 K) superconducting single-photon detectors (SSPDs)[20] have very low noise, even less than 100 counts per second, low time jitter (about 30 ps), and they can achieve high count rates, up to tens of megacounts per second; nevertheless, their active area is small (10×10 μm), they require bulky cryostats, and they are very expensive. InGaAs/InP single-photon avalanche diodes (SPAD)[21] have the typical advantages of solid-state devices as small size, low bias voltage, low power consumption, ruggedness, and reliability. Their photon detection efficiency is high (more than 20%) up to a wavelength of 1.7 μm and the dark count rate is a few thousand counts per seconds (cps) at the working temperature of 230 K. InGaAs/InP SPADs are commercially available with active area diameters up to 40 μm and their photon-timing jitter is lower than 100 ps. Moreover, they can be fast-gated because no damage occurs in the case of a strong photon flux and they are thus suitable for performing measurements at null interfiber distance.[22]

In this paper we present a new compact system for performing time-domain diffuse optical spectroscopy in the spectral range from 1100 nm to 1700 nm. As light source we chose a pulsed supercontinuum fiber laser, and a prism was used to disperse radiation. Moreover, to overcome the limitations intrinsic to using an MCP-PMT, which due to high cost and cooling requirements is basically confined to the laboratory, a time-gated InGaAs/InP SPAD has been employed, together with its driving module. Below, a description of our setup is reported, together with a characterization of the system performance and a first example of application.

MATERIALS AND METHODS

Experimental Setup. In the following the experimental setup employed for time-resolved near-infrared spectroscopy up to 1700 nm is described: in Fig. 1 a schematic of the system is depicted. Illumination is supplied by a photonic crystal fiber laser (SC450, Fianium, UK) emitting supercontinuum radiation in the spectral range 450–1750 nm with an overall power of 6 W. The laser pulses are provided at a repetition rate of 40 MHz, with duration of tens of picoseconds. Wavelength selection is achieved by means of the computer-controlled rotation of an F2-glass Pellin–Broca prism (Bernhard Halle Nachfl., GmbH, Berlin, Germany). The dispersed light is focused onto an adjustable slit, acting as a band-pass filter, thanks to an achromatic doublet with focal length of 150 mm (AC254-150-C-ML, Thorlabs, Germany). The radiation is subsequently coupled into a 100 μm core graded-index fiber by means of two achromatic doublets with focal lengths of 45 mm and 25 mm, respectively (AC254-045-B-ML and AC127-025-C-ML, Thorlabs, Germany) and sent to the sample. To attain a precise alignment of the fiber, a three-dimensional translational stage

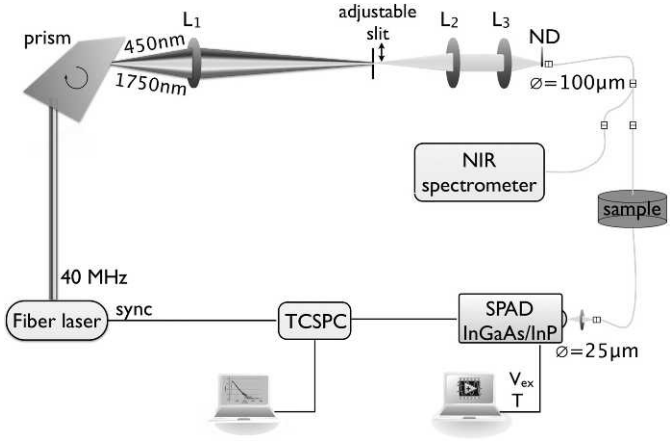

FIG. 1. Block diagram of the experimental setup for time-domain diffuse optical spectroscopy up to 1700 nm: the light source is a supercontinuum fiber laser, radiation is dispersed by a prism and diffused light is sent to an InGaAs/InP single photon avalanche diode.

in combination with a two-axis tilt is employed. The power on the sample can be adjusted by means of a motorized circularly variable neutral-density filter placed in front of the fiber. Figure 2 shows examples of normalized spectra in the range 1100–1700 nm and the respective powers obtained: the FWHM increases from 6.6 nm to 20.7 nm for increasing wavelengths because of the nonlinear dispersion of the prism, while the power at the probe is influenced by the source spectrum, the wavelength-dependent optical losses, and the fiber coupling efficiency. The possibility of accomplishing the wavelength selection through an acousto-optic tunable filter (AOTF) instead of using a prism was also considered, but the resulting spectra presented troublesome side lobes that affected the spectral purity and caused undesired effects during data analysis because of the different absorption experienced by the light at the wavelengths contained in such lobes.[23] Light diffused through the sample is collected using a 1 mm core

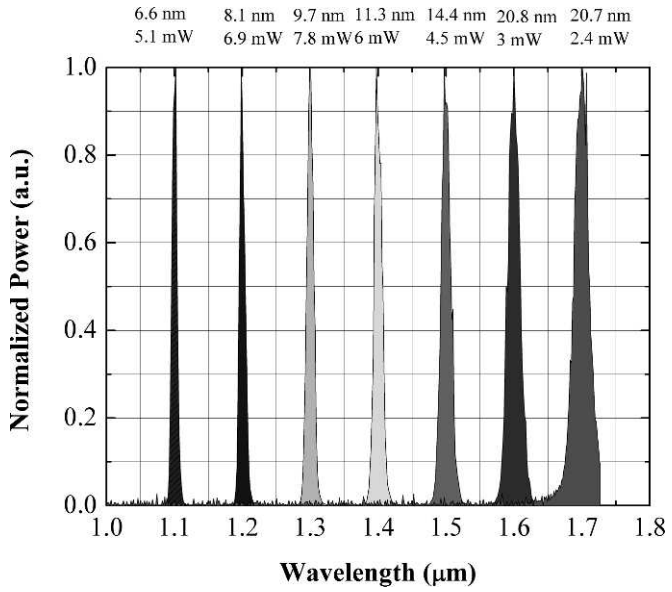

FIG. 2. Normalized spectral responses measured with a spectrometer in the range 1100–1700 nm at 7 different selected wavelengths (in steps of 100 nm). Optical powers were obtained with a powermeter.

multimodal step-index fiber and then focused on the active area of the detector, a time-gated InGaAs/InP SPAD characterized by a sensitivity spectral range extending from 900 nm to 1700 nm. Even if the active area has a diameter of only 25 μm, this detector is very suitable to reveal single-photon signals due to its high efficiency.[21] The detector is computer controlled by means of homemade software written in LabVIEW (National Instruments, USA) in order to set the required operating conditions (e.g., excess bias voltage, device temperature, gate_ON time, hold off time, etc.). The InGaAs/InP SPAD is operated at 230 K with gate duration of 10 ns and the overall temporal resolution of the system is around 150 ps (FWHM). The signal from the detector is driven to a time-correlated single-photon counting (TCSPC) board (SPC-130, Becker & Hickl, Germany) together with the synchronization signal, coming directly from the laser. To allow for fast measurement time and high reproducibility, the acquisition of the time-resolved curves is completely automated, even concerning wavelength selection and power attenuation, thanks to homemade software written in C language using the Lab Windows – CVI environment (National Instruments, USA).

Samples. To perform a test on the linearity of the system with respect to absorption and to check its capability to retrieve optical properties of extremely absorbing media, a liquid phantom was prepared using a stock solution of water and Intralipid® whose concentration was chosen to obtain a nominal reduced scattering coefficient μ_s' of about 15 cm^{-1} at 800 nm.[24] Afterwards, calibrated quantities of Indian Ink® were added in separate steps to gradually increase the absorption coefficient μ_a. Indian Ink® is a suspension of carbon micro-particles and at infrared wavelengths it shows a rather flat absorption spectrum.[25] Measurements were carried out at 1100 nm because for longer wavelengths water absorption is high enough to severely affect the optical signal. However, since the system is linear in time and the instrumental response function (IRF) does not change significantly with the wavelength as shown in Fig. 3 (described in more detail in the following), we expect no major difference in the behavior of the system at 1100 nm or at 1700 nm. A bandpass filter centered at 1100 nm and with a bandwidth of 10 nm was placed in front of the optical fiber before injecting the light into the sample. Reflectance geometry was employed, using an interfiber distance of 1 cm. For every ink concentration we performed six measurements lasting 30 s each. From these six measurements the mean absorption and reduced scattering values were retrieved and the standard deviation was calculated.

To test the linearity of the system for the scattering coefficient as well, another liquid phantom was prepared: calibrated quantities of Intralipid were added in separate steps to a stock solution of water to gradually increase its scattering coefficient. As for the measurements described above, measurements were performed at 1100 nm in reflectance configuration with the same bandpass filter as before with an interfiber distance of 1 cm. For every Intralipid concentration six measurements of 30 s each were obtained and from these the mean absorption and reduced scattering values were recovered, along with their respective standard deviation.

As a first example of application, a sample of lipids in a solid state (pig fat) was characterized. Lipids are an important constituent of biological tissues and a good knowledge of their spectrum is vital for correct quantification of tissue components. Pig fat was placed into a rectangular container (12.5 cm × 7 cm × 7 cm) with the upper side open: the sample was measured in reflectance geometry using an aluminum probe to hold the optical fibers in place. The interfiber distance was 1.25 cm. Measurements were performed in the spectral range 1100–1700 nm, in steps of 5 nm, and with acquisition time fixed at 60 s per wavelength.

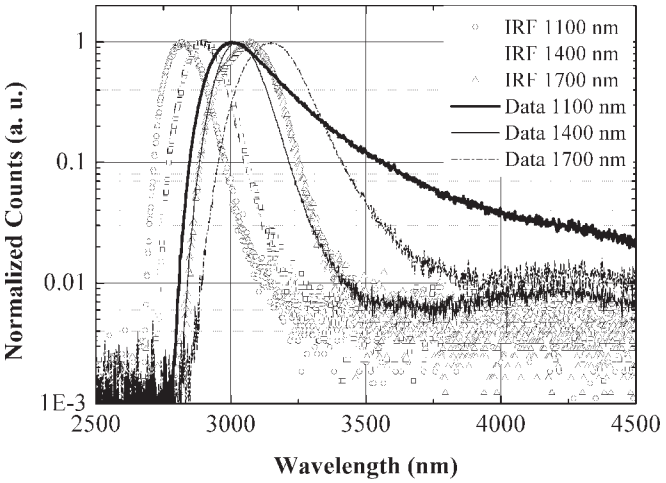

FIG. 3. Typical example of experimental data: open circles are the IRF obtained at 1100 nm (FWHM of 144 ps), open squares represent the IRF at 1400 nm (FWHM of 153 ps), and open triangles are the IRF at 1700 nm (FWHM of 205 ps); data curves obtained at these wavelengths are also reported: the thick solid line corresponds to the curve at 1100 nm (absorption coefficient 0.03 cm^{-1}, reduced scattering coefficient 4.23 cm^{-1}, FWHM 264 ps), the thin solid line represents the curve at 1400 nm (absorption coefficient 1.13 cm^{-1}, reduced scattering coefficient 5.55 cm^{-1}, FWHM 174 ps), and the dashed line is the curve taken at 1700 nm (absorption coefficient 0.25 cm^{-1}, reduced scattering coefficient 1.14 cm^{-1}, FWHM 233 ps).

Time-Resolved Data Analysis. Since in this spectral region we expected high absorption values for which the diffusion theory may not prove to be accurate, we exploited a method of analysis relying on the fitting of the experimental data to Monte Carlo (MC) simulations:[26] in the following it will be referred to as the Monte Carlo method (MCM). The code adopted is based on a work of 1998 where both the reflectance and the transmittance geometry were taken into account.[27] As a first step, a library of MC simulations at different scattering coefficients and zero absorption was generated by means of a CUDA® accelerated Monte Carlo code.[28] Pivot simulations were obtained simulating curves at different scattering values according to a geometric progression, in order to have a denser sampling for low scattering values and a less dense sampling for higher scattering values. To obtain a simulation at an arbitrary reduced scattering and absorption coefficient, a linear interpolation between pivot simulations was performed, followed by the multiplication for the factor $e^{-\mu_a v t}$ (where v is the speed of light), to account for the absorption in agreement with the radiative transfer equation. The simulated curve was then convoluted to the IRF and a Levenberg–Marquardt optimization procedure was performed. This analysis method has been used in many fields where a high absorption of the sample is involved, e.g., for in vivo medical spectroscopy, or for samples of finite dimensions.[29]

To understand how much the diffusion theory deviated from the correct prediction, in the case of the linearity measurements data were also analyzed with the diffusion approximation to the radiative transport equation: the optical properties, in terms of absorption and reduced scattering coefficients (μ_a and μ_s',

respectively), were retrieved for each wavelength by fitting the experimental data to an analytical solution of the diffusion approximation of the transport equation, with extrapolated boundary conditions for an infinite homogeneous slab;[30] we refer to this approach as to the diffusion method (DM). The theoretical curve was previously convoluted with the IRF to take into account its finite width, mainly arising from the width of the light pulse, the finite response of the detector, and the optical fiber dispersion. This fitting procedure is based only on the shape of the curves and not on their amplitude. To obtain a more robust procedure, the fitting range was set not to include the points of the time-resolved curves with a number of counts lower than 10% of the peak value on the rising edge and 1% on the tail. The fitting process is based on a standard Levenberg–Marquardt algorithm.[31]

For both methods a time shift between the reference and the data curve was introduced. This factor was not set as a free fitting parameter, but rather it was kept fixed to an optimum value: the optimum was found fitting the shift together with the absorption and scattering coefficients for the data curve with the lowest absorption.[32]

Figure 3 shows an example of the time-resolved curves obtained: the IRF at 1100 nm (open circles) has a FWHM of 144 ps, the IRF at 1400 nm (open squares) displays a FWHM of 153 ps, and the IRF curve at 1700 nm (open triangles) is characterized by a FWHM of 205 ps. The graph also displays experimental data curves acquired at these discrete wavelengths: the sample is characterized by an absorption coefficient and a reduced scattering coefficient of 0.03 cm^{-1} and 4.2 cm^{-1} at 1100 nm (thick solid line), of 1.1 cm^{-1} and 5.6 cm^{-1} at 1400 nm (thin solid line), and of 0.3 cm^{-1} and 1.14 cm^{-1} at 1700 nm (dashed line), respectively. The FWHM of the data curves are 264 ps for the curve taken at 1100 nm, 174 ps for 1400 nm, and 233 ps for 1700 nm. Typically the FWHM of diffused curves ranges from 160 ps to 260 ps.

RESULTS AND DISCUSSION

Linearity. In this section the results concerning the measurements performed on the calibrated solution of water, Intralipid, and Indian Ink are presented. Data were taken at 1100 nm. Figure 4 shows the absorption and reduced scattering coefficients as a function of Ink concentration retrieved both with the DM (top two panels) and with the MCM (bottom two panels). The good performance of the system in the assessment of low absorption values has already been proven.[33] Thus, we relied on the results obtained for low μ_a values to derive nominal μ_a values at high ink concentrations. In Figs. 4a and 4c, which refer to the absorption coefficient, the solid line represents the interpolation of the first seven values obtained with the DM and the MCM, respectively, and it is assumed to represent the theoretical absorption value of the solution. As can be seen, according to the analysis performed using the DM quite surprisingly the system displays a good linearity up to 0.025 mg/L of ink, which corresponds to a measured absorption value $\mu_a = 2.1$ cm^{-1}, and a displacement from the linear trend in terms of relative error (defined as the difference between the measured value and the theoretical value divided by the theoretical value) smaller than 27%. At higher ink concentrations, although the displacements become greater, there is no saturation of the values. The error bars, which represent the standard deviation, are negligible up to an estimated absorption value of 2.6 cm^{-1}, with a relative error of 29% and a standard deviation about 23%. The standard deviation increases with the ink concentration since the measures become more and more prohibitive and the data curve progressively approaches the IRF. It is worth noting that the first value on the graph, pertaining to the solution with only water and Intralipid and null concentration of ink, is in agreement with the range of values reported in the literature.[34–38] With the MCM the range in which a good linearity can be assumed is much higher: up to 0.037 mg/L of ink concentration (2.6 cm^{-1} of measured absorption) the displacement from the linear trend is negligible (3% in terms of relative error) and the standard deviation remains below 32%; upon increasing the ink content, the relative error is still below 20% (at 3.4 cm^{-1} of measured absorption the relative error is 17%) and no saturation of the absorption is present.

The reduced scattering coefficient for both the methods of analysis is reported in Figs. 4b and 4d: the straight dashed line indicates the mean value of the first seven measured values of μ_s' obtained with the DM and the MCM, respectively. As for the absorption, also here the standard deviations become greater for higher ink content. According to the DM, the higher the absorption of the solution, the more distant the data from the mean value, reaching the maximum relative error of 70% at 0.05 mg/L of ink. Conversely, applying the MCM the values obtained are closer to the mean value, with maximum relative error of only 22%, and the standard deviation is smaller if compared to the respective values obtained with the other method.

Figure 5 shows the absorption and reduced scattering coefficients as a function of the Intralipid concentration obtained at 1100 nm. Since for the linearity measurements in absorption the MC method proved more accurate in recovering the optical parameters, data were analyzed only with the MC procedure. On the left is displayed the reduced scattering coefficient; the dashed line represents the theoretical values expected: it is the interpolation of the last seven data points, those characterized by the highest scattering and therefore those for which we are sure of obtaining reliable results.[33] The good linearity of the system is well preserved down to an Intralipid concentration of 0.04 g/L, corresponding to a measured reduced scattering coefficient of 4.5 cm^{-1}: here the relative error is 18% and the standard deviation is 13%. As for the linearity in absorption, no saturation trend can be noticed and even for the very low value of 0.03 g/L of Intralipid (i.e., a measured μ_s' of 3.7 cm^{-1}) the relative error remains below 40% and the standard deviation is 15%.

The absorption coefficient is on the right side of Fig. 5. The straight solid line represents the mean value of the last seven data points. As the scattering properties of the solution decrease, the broadening of the temporal pulse is less pronounced with respect to the IRF of the system and therefore the measurements become more difficult. Anyway, the relative error is always below 7.5% and the maximum standard deviation is 0.5%.

We can conclude that the system presented here, together with the analysis procedures described above, has the necessary characteristics to analyze diffusive media with extremely high absorption and very low scattering and to retrieve reasonable estimates of both μ_a and μ_s'. These results have been exploited as a validation test for the measurements performed on the lipid sample. Compared to the expected results, the diffusion theory could also recover reasonable optical parameters, even at very high absorption values.

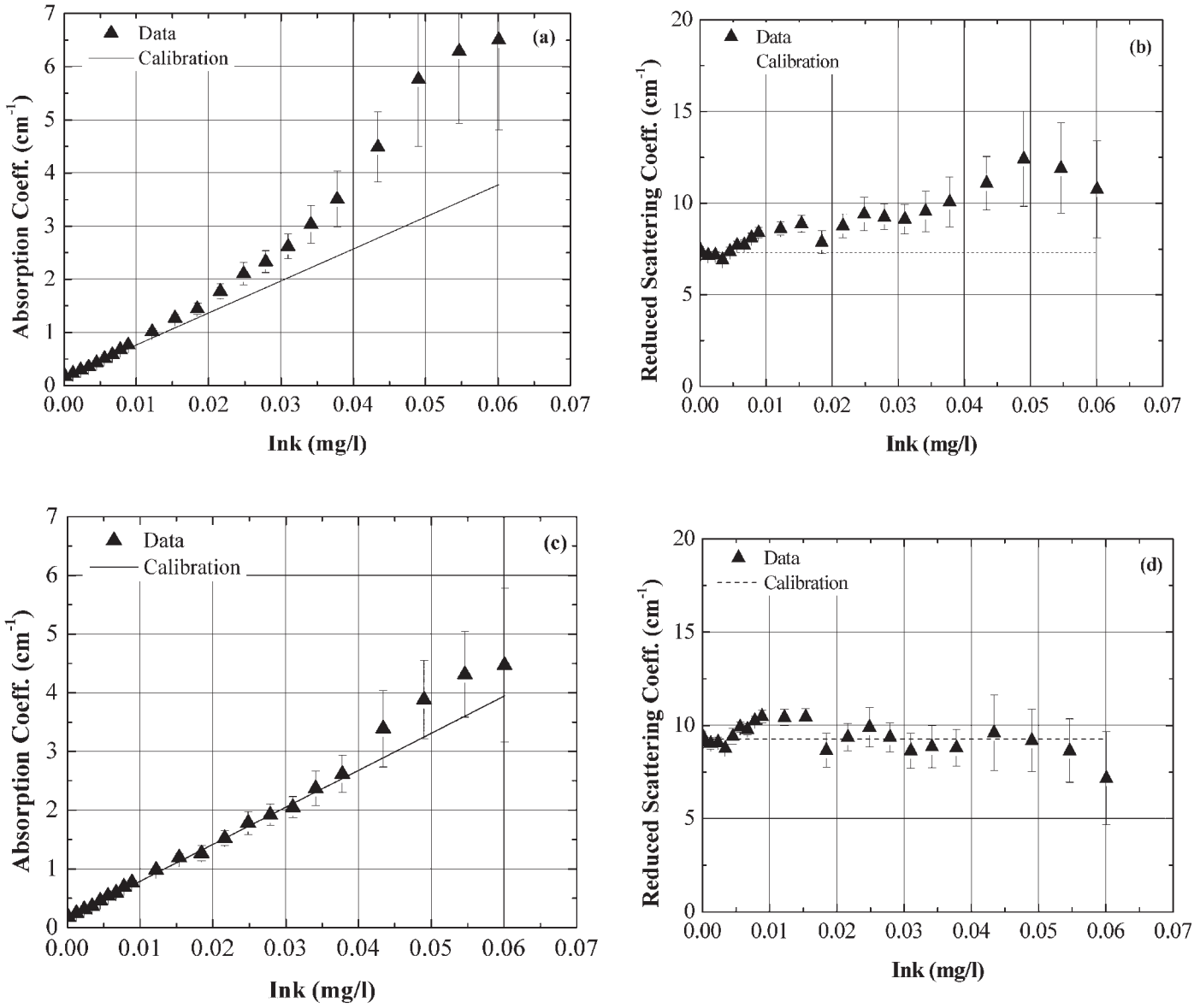

FIG. 4. Measurements performed on the liquid phantom of water, Intralipid®, and Indian Ink® taken at 1100 nm and analyzed either with the diffusion theory (**a, b**) or the Monte Carlo method (**c, d**). The absorption values retrieved as a function of ink concentration are reported in (**a**) and (**c**): the solid line is the linear interpolation of the first seven data points; the reduced scattering coefficient as a function of ink concentration is in (**b**) and (**d**): the dashed line represents the mean of the first seven points.

Anyway, for the measurements performed on the lipid sample we employed only the MCM since this method provided better results in terms of linearity and of smaller deviations.

Lipid Measurement. As a first example of application we have focused on the optical characterization of lipids (pig fat). Data were analyzed with the MCM. Figure 6 shows the reconstructed spectra for μ_a of the sample. The main features displayed by the absorption spectrum are three major peaks around 1200 nm, 1400 nm, and 1700 nm, respectively. The maximum absorption value is 1.09 cm^{-1}, reached around 1200 nm: this is an extremely high value, critical to the success of the measurements themselves, since it drastically limits the signal from the sample. However, we are confident in this result based on the linearity measurements reported above. In the figure is also shown the spectrum of lipids as reported by Nachabè et al.:[6] it was measured in the liquid phase with a spectrophotometer after melting the fat. As can be seen, data obtained with the time-resolved system working up to 1700 nm are in agreement with data acquired by another group and with a different system, a further confirmation of the reliability of our instrument.

Figure 7 shows the reduced scattering spectrum of lipids: it ranges from 4 cm^{-1} to 1 cm^{-1} in the wavelength range 1100–1700 nm. As expected from the measurements on linearity in scattering, there is some residual coupling between the reduced scattering coefficient and the absorption coefficient: this might be attributed to the relatively small interfiber distance (1.25 cm^{-1}) and the very low scattering values.

CONCLUSION

We described a new system capable of performing time-resolved diffuse optical spectroscopy up to 1700 nm. In this spectral region the absorption of the main constituents of

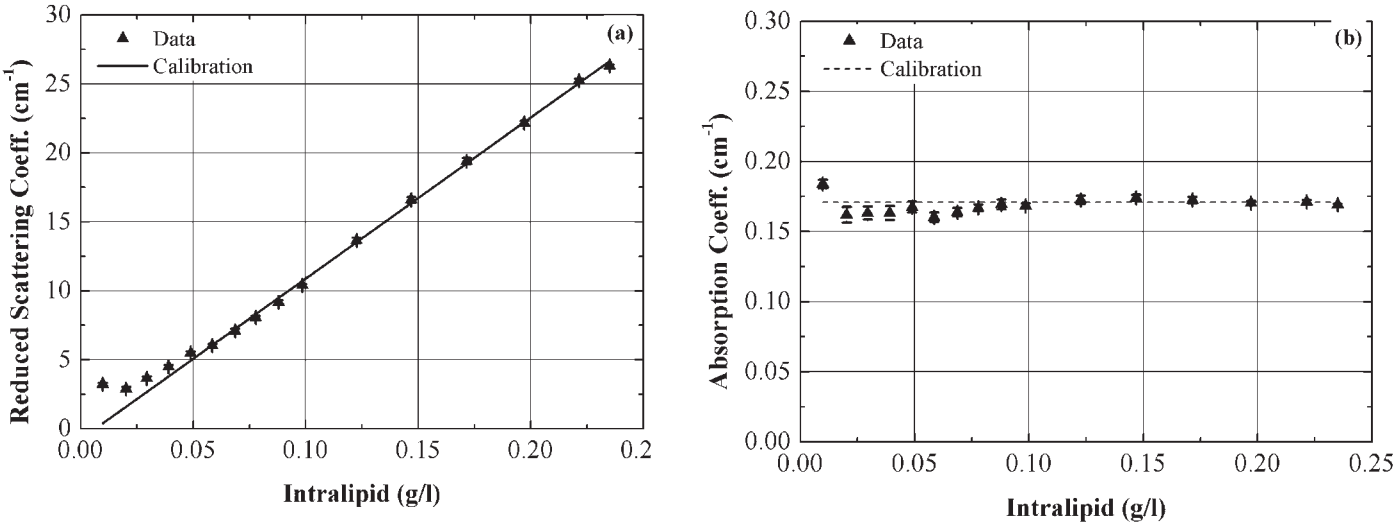

FIG. 5. Measurements performed on the liquid phantom of water and Intralipid® analyzed with a Monte Carlo method. Data were taken at 1100 nm. The reduced scattering values retrieved as a function of Intralipid® concentration are reported in (**a**): the solid line is the linear interpolation of the last seven data points; the reduced scattering coefficient as a function of Intralipid® concentration is in (**b**): the dashed line represents the mean of the last seven points.

biological tissues as well as many other materials is very high. With our system, based on a time-gated InGaAs/InP SPAD exploited together with a pulsed supercontinuum light source and a prism for wavelength selection, the feasibility to work in the spectral range 1100–1700 nm has been demonstrated: firstly a measurement on a calibrated liquid phantom has been presented, showing how at 1100 nm the system is linear in absorption up to 3.4 cm^{-1} and in scattering down to 4.5 cm^{-1}; since the system is time-invariant and the IRF does not change significantly with the wavelength, it can be assumed that the linear behavior extends up to 1700 nm. Then, a first example of a lipids spectrum has been shown: its absorption reaches up to 1.09 cm^{-1} around 1200 nm. To obtain better results, partially overcoming the limitations due to the model for high absorption values, a Monte Carlo fitting procedure was exploited. Remaining deviations between experimental data and real spectra may be attributed to non-idealities in the measurements themselves, such as possible drifts of the instrumental response function and spectral bandwidth effects. Furthermore, intrinsic instabilities of the fitting procedure can take place in case of extremely high absorption values. Future work will be carried out to further reduce the spectral bandwidth to avoid possible distortions of the spectra and to improve the performance of the InGaAs/InP SPAD module, in order to achieve higher count rates and stronger signal-to-noise ratio. Another future aim is to perform in vivo measurements on healthy volunteers to estimate tissue chromophore concentrations, including collagen, which is one of the main tissue components. Finally, we plan to test a wider range of materials, such as powders of pharmaceuticals or food of interest.

ACKNOWLEDGMENTS

The research leading to these results has received funding from the EC's Seventh Framework Programme (FP7/2007/2013) under grant agreements n. 228334, from the Ministero dell'Istruzione e dell'Università e della Ricerca of the Republic of Italy, and by the Swedish Council under the "Executive Programme for Scientific and Technological Cooperation between Italy and

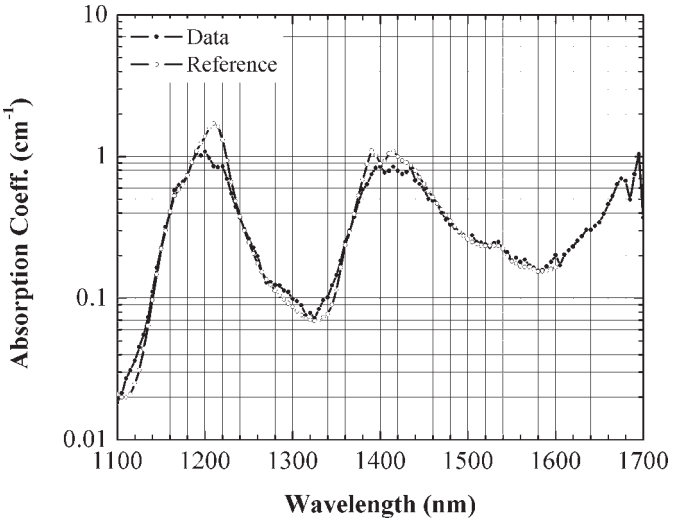

FIG. 6. Absorption spectrum of lipids as a function of wavelength (solid dots); also displayed is the lipids spectrum as reported by Nachabè et al.[6] (open dots).

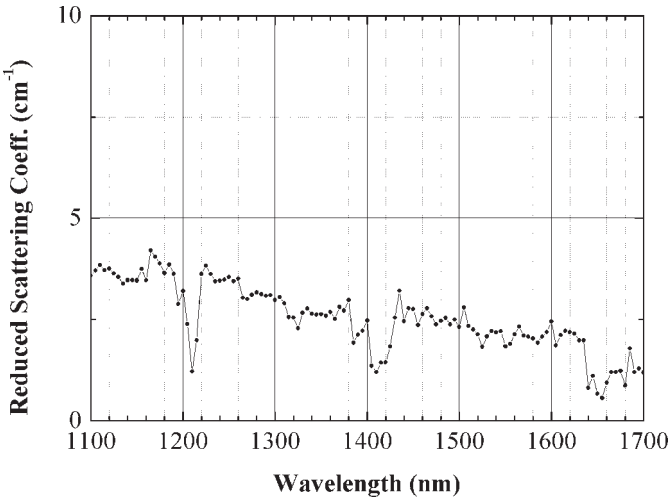

FIG. 7. Reduced scattering coefficient of the lipids spectrum as a function of wavelength.

Sweden". It has also been supported by the Italian Ministero dell'Istruzione dell'Università e della Ricerca under PRIN project 2009XT785A_002.

1. R.M.P. Doornbos, R. Lang, M.C. Aalders, F.W. Cross, H.J.C.M. Sterenborg. "The Determination of in vivo Human Tissue Optical Properties and Absolute Chromophore Concentrations Using Spatially Resolved Steady-State Diffuse Reflectance Spectroscopy". Phys. Med. Biol. 1999. 44: 967-981.
2. T.H. Pham, F. Bevilacqua, T. Spott, J.S. Dam, B.J. Tromberg, S. Andersson-Engels. "Quantifying the Absorption and Reduced Scattering Coefficients of Tissuelike Turbid Media Over a Broad Spectral Range with Noncontact Fourier-Transform Hyperspectral Imaging". Appl. Opt. 2000. 39(34): 6487-6497.
3. T.H. Pham, O. Coquoz, J.B. Fishkin, E. Anderson, B.J. Tromberg. "Broad Bandwidth Frequency Domain Instrument for Quantitative Tissue Optical Spectroscopy". Rev. Sci. Instrum. 2000. 71(6): 2500-2513.
4. F. Bevilacqua, A.J. Berger, A.E. Cerussi, D. Jakubowski, B.J. Tromberg. "Broadband Absorption Spectroscopy in Turbid Media by Combined Frequency-Domain and Steady-State Methods". Appl. Opt. 2000. 39(34): 6498-6507.
5. L. Spinelli, F. Martelli, A. Farina, A. Pifferi, A. Torricelli, R. Cubeddu, G. Zaccanti. "Calibration of Scattering and Absorption Properties of a Liquid Diffusive Medium at NIR Wavelengths. Time-Resolved Method". Opt. Exp. 2007. 15(11): 6589-6604.
6. R. Nachabé, B.H. Hendriks, A.E. Desjardins, M. van der Voort, M.B. van der Mark, H.J. Sterenborg. "Estimation of Lipid and Water Concentrations in Scattering Media with Diffuse Optical Spectroscopy from 900 to 1600 nm". J. Biomed. Opt. 2010. 15(3): 037015. doi: 10.1117/1.3454392.
7. G. Nishimura, I. Kida, M. Tamura. "Characterization of Optical Parameters with a Human Forearm at the Region from 1.15 to 1.52 μm Using Diffuse Reflectance Measurements". Phys. Med. Biol. 2006. 51: 2997-3011.
8. M.S. Patterson, B. Chance, B.C. Wilson. "Time Resolved Reflectance and Transmittance for the Non-Invasive Measurement of Tissue Optical Properties". Appl. Opt. 1989. 28(12): 2331-2336.
9. S. Andersson-Engels, R. Berg, A. Persson, S. Svanberg. "Multispectral Tissue Characterization with Time-Resolved Detection of Diffusely Scattered White Light". Opt. Lett. 1993. 18(20): 1697-1699.
10. A. Pifferi, A. Torricelli, P. Taroni, D. Comelli, A. Bassi, R. Cubeddu. "Fully Automated Time Domain Spectrometer for the Absorption and Scattering Characterization of Diffusive Media". Rev. Sci. Instrum. 2007. 78: 053103. doi: 10.1063/1.2735567.
11. C. Abrahamsson, T. Svensson, S. Svanberg, S. Andersson-Engels, J. Johansson, S. Folestad. "Time and Wavelength Resolved Spectroscopy of Turbid Media Using Light Continuum Generated in a Crystal Fiber". Opt. Exp. 2004. 12(17): 4103-4112.
12. A. Bassi, J. Swartling, C. D'Andrea, A. Pifferi, A. Torricelli, R. Cubeddu. "Time-Resolved Spectrophotometer for Turbid Media Based on Supercontinuum Generation in a Photonic Crystal Fiber". Opt. Lett. 2004. 29(20): 2405-2407.
13. S. Tsuchikawa, S. Tsutsumi. "Application of Time-of-Flight Near-Infrared Spectroscopy to Wood with Anisotropic Cellular Structure". Appl. Spectrosc. 2002. 56(7): 869-876.
14. T. Svensson, E. Alerstam, D. Khoptyar, J. Johansson, S. Folestad, S. Andersson-Engels. "Near-Infrared Photon Time-of-Flight Spectroscopy of Turbid Materials up to 1400 nm". Rev. Sci. Instrum. 2009. 80: 063105. doi: 10.1063/1.3156047.
15. T. Svensson, E. Adolfsson, M. Lewänder, C. Xu, S. Svanberg. "Disordered, Strongly Scattering Porous Materials as Miniature Multipass Gas Cells". Phys. Rev. Lett. 2011. 107: 143901. doi: 10.1103/PhysRevLett.107.143901.
16. A. Tosi, A. Della Frera, A. Bahgat Shehata, C. Scarcella. "Fully Programmable Single-Photon Detection Module for InGaAs/InP Single-Photon Avalanche Diodes with Clean and Sub-Nanosecond Gating Transitions". Rev. Sci. Instrum. 2012. 83: 013104. doi: 10.1063/1.3675579.
17. W. Becker. "Photon Counting Performance of Selected Detectors". In: A.W. Castleman, Jr., J.P. Toennies, W. Zinth, editors. Advanced Time-Correlated Single-Photon Counting Techniques. Berlin, Germany: Springer, 2005. Chap. 6.4.1, Pp. 243-244.
18. Hamamatsu Photonics. Japan. http://sales.hamamatsu.com/assets/pdf/parts_R/R3809U-68_-69_TPMH1293E03.pdf [accessed May 7 2012].
19. Hamamatsu Photonics. Japan: . "Guide to Streak Cameras, 2002. http://sales.hamamatsu.com/assets/pdf/hpspdf/Guidetostreak.pdf [accessed May 7 2012].
20. G.N. Gol'tsman, O. Okunev, G. Chulkova, A. Lipatov, A. Dzardanov, K. Smirnov, A. Semenov, B. Voronov, C. Williams, R. Sobolewski. "Fabrication and Properties of an Ultrafast NbN Hot-Electron Single-Photon Detector". IEEE Trans. On Applied Superconductivity. 2001. 11(1): 574-577.
21. A. Tosi, A. Dalla Mora, F. Zappa, S. Cova. "Single-Photon Avalanche Diodes for the Near-Infrared Range: Detector and Circuit Issues". J. Mod. Opt. 2009. 56: 299-308.
22. A. Pifferi, A. Torricelli, L. Spinelli, D. Contini, R. Cubeddu, F. Martelli, G. Zaccanti, A. Tosi, A. Dalla Mora, F. Zappa, S. Cova. "Time-Resolved Diffuse Reflectance Using Small Source-Detector Separation and Fast Single-Photon Gating". Phys. Rev. Lett. 2008. 100: 138101. doi: 10.1103/PhysRevLett.100.138101.
23. A. Farina, A. Bassi, A. Pifferi, P. Taroni, D. Comelli, L. Spinelli, R. Cubeddu. "Bandpass Effects in Time-Resolved Diffuse Spectroscopy". Appl. Spectrosc. 2009. 63(1): 48-56.
24. L. Spinelli, F. Martelli, A. Farina, A. Pifferi, A. Torricelli, R. Cubeddu, G. Zaccanti. "Calibration of Scattering and Absorption Properties of a Liquid Diffusive Medium at NIR Wavelengths. Time-Resolved Method". Opt. Exp. 2007. 15(11): 6589-6604.
25. P. Di Ninni, F. Martelli, G. Zaccanti. "The Use of India Ink in Tissue-Simulating Phantoms". Opt. Exp. 2010. 18(26): 26854-26865.
26. E. Alerstam, S. Andersson-Engels, T. Svensson. "Improved accuracy in time-resolved diffuse reflectance spectroscopy". Opt. Exp. 2008. 16(14): 10440-10454.
27. A. Pifferi, P. Taroni, G. Valentini, S. Andersson-Engels. "Real-Time Method for Fitting Time-Resolved Reflectance and Transmittance Measurements with a Monte Carlo Model". Appl. Opt. 1998. 37(13): 2774-2780.
28. E. Alerstam, T. Svensson, S. Andersson-Engels. "Parallel Computing with Graphics Processing Units for High-Speed Monte Carlo Simulation of Photon Migration". J. Biomed. Opt. 2008. 13(6): 060504. doi: 10.1117/1.3041496.
29. J.-P. Bouchard, I. Veilleux, R. Jedidi, I. Noiseux, M. Fortin, O. Mermut. "Reference Optical Phantoms for Diffuse Optical Spectroscopy. Part 1–Error Analysis of a Time Resolved Transmittance Characterization Method". Opt. Exp. 2010. 18(11): 11495-11507.
30. D. Contini, F. Martelli, G. Zaccanti. "Photon Migration Through a Turbid Slab Described by a Model Based on Diffusion Approximation. I. Theory". Appl. Opt. 1997. 36(19): 4587-4599.
31. W.H. Press, S.A. Teukolsky, W.T. Vetterling, B.P. Flannery. Numerical Recipes in C: the Art of Scientific Computing. Cambridge, UK: Cambridge University Press, 1992.
32. R. Cubeddu, A. Pifferi, P. Taroni, A. Torricelli, G. Valentini. "Experimental Test of Theoretical Models for Time-Resolved Reflectance". Med. Phys. 1996. 23(9): 1625-1633.
33. A. Pifferi, A. Torricelli, P. Taroni, D. Pomelli, A. Bassi, R. Cubeddu. "Fully Automated Time Domain Spectrometer for the Absorption and Scattering Characterization of Diffusive Media". Rev. Sci. Instrum. 2007. 78: 053103. doi: 10.1063/1.2735567.
34. L. Kou, D. Labrie, P. Chylek. "Refractive Indices of Water and Ice in the 0.65-2.5 μm Spectral Range". Appl. Opt. 1993. 32: 3531-3540.
35. G.M. Hale, M.R. Quarry. "Optical Constants of Water in the 200 nm to 200 μm Wavelength Region". Appl. Opt. 1973. 12: 555-563.
36. M.R. Quarry, P.G. Cary, R.C. Waring. "Split-Pulse Laser Method for Measuring Attenuation Coefficients of Transparent Liquids: Application to Deionized Filtered Water in the Vsible Region". Appl. Opt. 1978. 17: 3587-3592.
37. K.F. Palmer, D. Williams. "Optical Properties of Water in the Near Infrared". J. Opt. Soc. Am. 1974. 64: 1107-1110.
38. W.M. Irvine, J.B. Pollack. "Infrared Optical Properties of Water and Ice Spheres". Icarus. 1968. 8: 324-360.